

Adaptive and Robust Watermark for Generative Tabular Data

Daniel Ngo¹, Daniel Scott^{*1}, Saheed Obitayo¹, Archan Ray², Akshay Seshadri², Niraj Kumar², Vamsi K. Potluru¹, Marco Pistoia², and Manuela Veloso¹

¹AI Research, JPMorganChase, New York, NY 10017, USA

²Global Technology Applied Research, JPMorganChase, New York, NY 10001, USA

{tuandung.ngo, saheed.obitayo, archan.ray, akshay.seshadri, niraj.x7.kumar, vamsi.k.potluru, marco.pistoia, manuela.veloso}@jpmchase.com

Abstract

Recent development in generative models has demonstrated its ability to create high-quality synthetic data. However, the pervasiveness of synthetic content online also brings forth growing concerns that it can be used for malicious purpose. To ensure the authenticity of the data, *watermarking* techniques have recently emerged as a promising solution due to their strong statistical guarantees. In this paper, we propose a flexible and robust watermarking mechanism for generative tabular data. Specifically, a data provider with knowledge of the downstream tasks can partition the feature space into pairs of *(key, value)* columns. Within each pair, the data provider first uses elements in the *key* column to generate a randomized set of “green” intervals, then encourages elements of the *value* column to be in one of these “green” intervals. We show theoretically and empirically that the watermarked datasets (i) have negligible impact on the data quality and downstream utility, (ii) can be efficiently detected, (iii) are robust against multiple attacks commonly observed in data science, and (iv) maintain strong security against adversary attempting to learn the underlying watermark scheme.

1 Introduction

With the recent development in generative models, synthetic data [Jordon et al., 2022] has become more ubiquitous with applications ranging from health care [Gonzales et al., 2023] to finance [Assefa et al., 2020, Potluru et al., 2023]. Among these applications, synthetic data can be an alternative option to human-generated data due to its high quality and relatively low cost. However, there is also a growing concern that carelessly adopting synthetic data with the same frequency as human-generated data may lead to misinformation and privacy breaches. Thus, synthetic data needs to be detectable by any upstream data-owner.

Watermarking has recently emerged as a promising solution to synthetic data detection with applications in generative text [Kirchenbauer et al., 2023, Kuditipudi et al., 2024], images [An et al., 2024], and relational data [He et al., 2024, Zheng et al., 2024]. A watermark is a hidden pattern embedded in the data that may be indiscernible to an oblivious human decision-maker, yet can be algorithmically detected through an efficient procedure. The watermark carries several desirable properties, notably: (i) **fidelity** - it should not degrade the quality and usability of the original dataset; (ii) **detectability** - it must be reliably identified through a specific detection

^{*}Work done while at AI Research, JPMorganChase

Key A	Value B	Value A	Key B
K_1	...	V_1	...
K_2	...	V_2	...
K_3	...	V_3	...

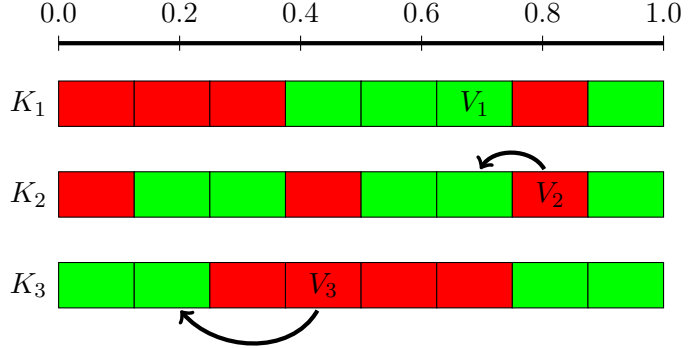


Figure 1: Illustrative example of Algorithm 1 on a tabular dataset with 3 rows and 4 columns. This structure corresponds to 2 pairs of $(key, value)$ columns. In the first row, the element V_1 is already in a ‘green’ bin. Meanwhile, the other elements, V_2 and V_3 , have to be moved from ‘red’ interval to a nearby ‘green’ interval.

process; (iii) **robustness** - it should withstand manipulations from an adversary [Katzenbeisser and Petitcolas, 2000, Atallah et al., 2001]; and (iv) **security** - it should be hard for an adversary to learn the exact parameters of the underlying watermarking scheme.

Applying a watermark to the synthetic tabular dataset is particularly challenging due to its structure. A tabular dataset must follow a specific format where each row contains a fixed number of features, i.e., precise information about an individual. Hence, even perturbation of a subset of features in the data can substantially affect the performance of downstream tasks. Furthermore, tabular data is commonly subjected to various methods of data manipulation by the downstream data scientist, e.g., feature selection and data alteration, to improve data quality and enable efficient learning. While prior works [He et al., 2024, Zheng et al., 2024] have proposed watermarking for tabular data, they often fail to address how their watermark performs under these innocuous attacks masked as preprocessing steps.

This paper focuses on establishing a theoretical framework for watermarking tabular datasets. Our approach leverages the structure of the feature space to form pairs of $(key, value)$ columns for a more fine-grained watermark embedding. The elements in the *key* columns are divided into consecutive intervals, whose centers determine the seed to generate random ‘red’ and ‘green’ intervals for the corresponding *value* columns. We embed the watermark into the data by promoting all elements in the *value* columns to fall into these green intervals. For an illustrative example of this watermarking process on a stylized dataset, see Figure 1. During the detection phase, we employ a hypothesis test to examine the characteristics of the empirical data distribution. Furthermore, we provide theoretical and empirical analysis of the watermark’s robustness to various oblivious attacks on synthetic and real-world datasets. Finally, we provide the first set of theoretical results on the query complexity for an adversary to learn the watermarking scheme. We summarize our main contributions as follows:

- In Section 4, we propose a fine-grained watermarking scheme for tabular data with strong statistical guarantees and desirable properties: fidelity, detectability, robustness, and security. To our knowledge, this is the first work that leverages the feature space structure to watermark tabular datasets.
- To enhance robustness and ensure high-quality data for downstream tasks, we employ a pairing subroutine based on the feature importance. Our proposed pairing scheme retains twice as many essential columns under the feature selection attack as the naive approach.

- In Section 7, we give an upper bound on the query complexity required by an adversary to learn our watermarking scheme under two querying schema: table-like queries and row-like queries. This is the first theoretical result on statistical learning of tabular watermarking techniques.
- In Section 8, we demonstrate our proposed watermarking method’s high fidelity, detectability, robustness and security on a set of synthetic and real-world datasets.

2 Related Work

Watermarking tabular data There exists a long line of research studying watermarking schemes for tabular data. Agrawal and Kiernan [2002] is the first work to tackle this problem setting, where the watermark was embedded in the least significant bit of some cells, i.e., setting them to be either 0 or 1 based on a hash value computed using primary and private keys. Subsequently, Xiao et al. [2007], Hamadou et al. [2011] proposed an improved watermarking scheme by embedding multiple bits. Another approach is to embed the watermark into the data statistics. Notably, Sion et al. [2003] partitioned the rows into different subsets and embedded the watermark by modifying the subset-related statistics. This approach is then improved upon by Shehab et al. [2007] to protect against insertion and deletion attacks by optimizing the partitioning algorithm and using hash values based on primary and private keys. To minimize data distortion, the authors modeled the watermark as an optimization problem solved using genetic algorithms and pattern search methods. However, this approach is strictly limited by the requirement for data distribution and the reliance on primary keys for partitioning algorithms.

Inspired by the recent watermarking techniques in large language models [Kamaruddin et al., 2018, Aaronson, 2023, Kuditipudi et al., 2024, Kirchenbauer et al., 2023], He et al. [2024] and Zheng et al. [2024] have made advances in watermarking generative tabular data by splitting the value range into red and green intervals. He et al. [2024] proposed a watermarking scheme through data binning, ensuring that all elements in the original data are close to a green interval. In conjunction with a statistical hypothesis test for detection, this embedding method allows the authors to protect the watermark from additive noise attack. However, the authors assumed that both the tabular dataset and the additive noise elements are sampled from a continuous distribution, which does not account for attacks such as feature selection or truncation. Zheng et al. [2024] instead only embedded the watermark in the prediction target feature. While the authors showed that this watermarking technique can handle several attacks and categorical features, their results primarily focused on watermarking one feature using a random seed, which is often insufficient in practice. In contrast, our technique guarantees that half of the dataset is watermarked with the seed chosen based on the data in *key* columns. As a result, our watermark approach is more robust to dataset-level manipulations such as feature subset attacks, especially when the target feature for downstream tasks is not known in advance. Moreover, we observe an interesting tradeoff between robustness and detection cost among these prior work and our approach: with the same level of fidelity, He et al. [2024]’s watermark is the easiest to detect but is less robust to oblivious and adversarial attacks compared to Zheng et al. [2024] and our watermarks. On the other hand, we focus on enhancing the robustness of the watermark against potential attacks at the cost of harder detection due to the need to recover the exact $(key, value)$ feature pairs. Finally, Zheng et al. [2024] offers a watermark algorithm that works for both continuous and categorical features with mildly higher detection cost and robustness compared to He et al. [2024]. For a high level summary of the comparison between our method and these two works, see Table 1.

Particularly, both the prior works [He et al., 2024, Zheng et al., 2024] and our proposed

approach maintain high data fidelity, measured by comparing the utility of using the watermarked dataset compared to the original unwatermarked dataset on downstream machine learning tasks. While all three approaches use a similar hypothesis testing procedure to detect the watermark, He et al. [2024]’s watermark is the easiest to detect. The additional cost of watermark detection in Zheng et al. [2024] and our schemes are due to the selection of the watermarked features. At detection time, the third-party need to identify either the target watermarked feature (for Zheng et al. [2024]’s watermark) or all (key, value) feature pairs (for our approach). Among all three approaches, ours is the most robust to oblivious attacks (details in Section 8) as our watermark scheme can withstand feature selection attacks, which is an improvement over prior work. For security attacks, we provide the first upper bound on query complexity required by an adversary to learn the watermark scheme. Under our analysis Section 7, this upper bound is the same for all three tabular watermarking approaches.

Tabular Watermark	Data Type	Fidelity \uparrow	Detection Cost \downarrow	Robustness \uparrow	Security
He et al. [2024]	Numerical	High	Low	Low	$\tilde{O}(mnb)$
Zheng et al. [2024]	Numerical, Categorical	High	Medium	Medium	$\tilde{O}(mnb)$
Ours	Numerical	High	High	High	$\tilde{O}(mnb)$

Table 1: A comparison of the data type and results from [He et al., 2024, Zheng et al., 2024] and our technique for watermarking generative tabular data. Although our method achieves high fidelity and robustness, it does not handle categorical data and suffers from high detection costs. There is no clear ‘winner’ as each paper focuses on improving a different watermark property.

3 Problem Formulation

Notation. For $n \in \mathbb{N}^+$, we write $[n]$ to denote $\{1, \dots, n\}$. For a matrix $\mathbf{X} \in \mathbb{R}^{m \times 2n}$, we denote the L -infinity norm of \mathbf{X} as $\|\mathbf{X}\|_\infty = \max_{i \in [m], j \in [2n]} |\mathbf{X}_{i,j}|$. For an interval $g = [a, b]$, we denote the center of g as $\text{center}(g) = (a+b)/2$.

In this paper, we consider an original tabular dataset $\mathbf{X} \in [0, 1]^{m \times 2n}$ with each column containing m i.i.d data points from a (possibly unknown) distribution $F_i, i \in [2n]$ with continuous probability density function f_i . Our main objective is to generate a watermarked version of this data, denoted \mathbf{X}_w , that achieves the following properties:

- (i) **Fidelity:** the watermarked dataset \mathbf{X}_w is close to the original data set \mathbf{X} to maintain high fidelity, measured through L_∞ distance and Wasserstein distance;
- (ii) **Detectability:** the watermarked dataset \mathbf{X}_w can be reliably identified through the one-proportion z -test using only few row samples;
- (iii) **Robustness:** the watermarked dataset \mathbf{X}_w achieves desirable robustness against multiple methods of oblivious ‘attack’ commonly observed in data science;
- (iv) **Security:** it is difficult for an adversary to learn the underlying watermarking scheme without considerable computational efforts.

Note that in our analysis, we only focus on embedding the watermark in the continuous features of a tabular dataset. While a real-world tabular dataset may contain many categorical features, embedding the watermark in these features through a small perturbation of its value may cause significant changes in the meaning for the entire sample (row). Given a dataset \mathbf{X} with both

Algorithm 1: Pairwise Tabular Watermarking

Input: Tabular dataset $\mathbf{X} \in \mathbb{R}^{m \times 2n}$. Number of bins $b \in \mathbb{N}^+$. Pairing subroutine PAIR.

Output: Watermarked dataset \mathbf{X}_w .

- 1: Divide the columns into n pairs of columns labeled $(key, value)$ using PAIR.
- 2: Divide the key columns into bins of equal width $1/b$ to form consecutive intervals denoted $\{I_j\}_{j \in [b]}$, where $I_j = [j-1/b, j/b]$.
- 3: **for** each key column **do**
- 4: Use the center of the bins to compute the hash and seed a random number generator.
- 5: Randomly generate red and green intervals, ensuring equal number of each type. Denote the set of green intervals as G .
- 6: **for** each element x in the paired $value$ column **do**
- 7: Identify the nearest green interval as $g = \arg \min_{g \in G} |x - \text{center}(g)|$.
- 8: **if** $x \notin g$ **then**
- 9: Replace x with x_w uniformly sampled from g .
- 10: **else**
- 11: Leave x as is.

categorical and continuous features, we can run our algorithm on a smaller dataset $\mathbf{X}' \subseteq \mathbf{X}$ with same number of rows and only continuous features. After the watermark has been embedded in \mathbf{X}' to get \mathbf{X}'_w , we reconstruct a watermarked version of the original dataset \mathbf{X} by replacing the continuous features of \mathbf{X} with its watermarked versions from \mathbf{X}'_w . We leave the study of watermarking categorical features in tabular datasets for future work.

4 Pairwise Tabular Data Watermark

In this section, we provide the details of the watermarking algorithm. At a high level, we embed the watermark into a tabular dataset \mathbf{X} by leveraging the pairwise structure of its feature space. Particularly, we first partition the feature space into pairs of $(key, value)$ columns using a subroutine PAIR. Detail of this subroutine will be discussed in the later section. Then, we finely divide the range of elements in each key column into bins of size $1/b$ to form b consecutive intervals. The center of the bins for each key column is then used to compute a hash, which becomes the seed for a random number generator. This random number generator then randomly generates red and green intervals for the corresponding $value$ column, where each interval is of size $1/b$. For simplicity, in the remaining analysis, we assume that half of the intervals is red (and the other half is green). Finally, we embed the watermark in elements of this $value$ column by ensuring that they are always in a nearby green interval with minimal distortion. This process is repeated until all $value$ columns are watermarked. We formally describe our proposed watermarking method in Algorithm 1 below.

4.1 Fidelity of Pairwise Tabular Data Watermark

First, we show that the watermarked dataset \mathbf{X}_w maintains high fidelity, i.e., \mathbf{X}_w is close to the \mathbf{X} in L_∞ distance. Since the red and green intervals are randomly assigned, our bound on the L_∞ distance holds with high probability. Intuitively, this bound depends on the distance to the nearest green interval: the probability that a search radius contains a green interval grows with the number of adjacent bins included in the search.

Theorem 4.1 (Fidelity). *Let $\mathbf{X} \in [0, 1]^{m \times 2n}$ be a tabular dataset, and \mathbf{X}_w is its watermarked version from Algorithm 1. With probability at least $1 - \delta$ for $\delta \in (0, 1)$, the L_∞ distance between*

\mathbf{X} and \mathbf{X}_w is upper bounded by:

$$\mathbb{E}[\|\mathbf{X}_w - \mathbf{X}\|_\infty] \leq \frac{\log_2(mn/\delta)}{b} \quad (1)$$

Theorem 4.1 gives rise to a natural corollary that upper bounds the Wasserstein distance, i.e., the distance between the empirical distributions of \mathbf{X} and \mathbf{X}_w . Together, Theorem 4.1 and Corollary 4.2 show that in expectation, the watermarked dataset \mathbf{X}_w is close to the original dataset \mathbf{X} . Thus, downstream tasks operated on \mathbf{X}_w instead of \mathbf{X} would only induce additional error in the order of $1/b$ with high probability. We empirically show the impact of this additional error for several synthetic and real-world datasets in Section 8.

Corollary 4.2 (Wasserstein distance). *Let $F_{\mathbf{X}} = \sum_{j=1}^m \delta_{\mathbf{X}[j,:]}$ be the empirical distribution built on $\mathbf{X} \in [0, 1]^{m \times 2n}$, and $F_{\mathbf{X}_w} = \sum_{j=1}^m \frac{1}{m} \delta_{\mathbf{X}_w[j,:]}$ be the empirical distribution built on \mathbf{X}_w . With probability at least $1 - \delta \in (0, 1)$, the k -Wasserstein distance is upper bounded by*

$$\mathcal{W}_k(F_{\mathbf{X}}, F_{\mathbf{X}_w}) \leq \frac{\sqrt{2n} \cdot \log_2(mn/\delta)}{b} \quad (2)$$

5 Detection of Pairwise Tabular Data Watermark

In this section, we provide the details of the watermark detection protocol. Informally, the detection protocol employs standard statistical measures to determine whether a dataset is watermarked with minimal knowledge assumptions. Particularly, we introduce the following lemma that shows, with an increasing number of bins, the probability of any element in a *value* column belonging to a green interval approaches $1/2$. That is, without running the watermarking algorithm 1, we have a baseline for the expected number of elements in green intervals for each *value* column.

Lemma 5.1. *Consider a probability distribution F with support in $[0, 1]$. As the number of bins $b \rightarrow \infty$, for each element x in a value column, we have $\Pr_{x \sim F}[x \in G] \rightarrow 1/2$.*

We formalize the process of detecting our watermark through a hypothesis test. Intuitively, the result of Lemma 5.1 implies that, for any *value* column, the probability of an element being in a green list interval is approximately $1/2$. While this convergence is agnostic to how the green intervals are chosen, it is non-trivial for a data-provider to detect the watermark due to the pairwise structure of Algorithm 1. Particularly, if the data-provider has knowledge of the *value* columns and the hash function, they still need to individually check which *key* column corresponds to the selected *value* column. In the worst case, all n *key* columns must be checked for each *value* column before the data-provider can confidently claim that the dataset is not watermarked. With this knowledge, we formulate the hypothesis test as follows:

Hypothesis test

$$\begin{aligned} H_0 &: \text{Dataset } X \text{ is not watermarked} & H_{0,i} &: \text{The } i\text{-th value column is not watermarked} \\ H_1 &: \text{Dataset } X \text{ is watermarked} & & \end{aligned}$$

That is, when the null hypothesis holds, all of the individual null hypotheses for the i -th value column must hold simultaneously. Thus, the data-owner who wants to detect the watermark for

a dataset \mathbf{X} would need to perform the hypothesis test for each *value* column individually. If the goal is to reject the null hypothesis H_0 when the p -value is less than a predetermined significant threshold α (typically 0.05 to represent 5% risk of incorrectly rejecting the null hypothesis), then the data-provider would check if the p -value for each individual null hypothesis $H_{0,i}$ is lower than α/n^2 (after accounting for the family-wise error rate using Bonferroni [Bonferroni, 1936]).¹

Let T_i denote the number of elements in the i -th *value* column that falls into a green interval. Then, under the individual null hypothesis $H_{0,i}$, we know that $T_i \sim B(m, 1/2)$ for large number of rows m . Using the Central Limit Theorem, we have $2\sqrt{m} \left(\frac{T_i}{m} - \frac{1}{2} \right) \rightarrow \mathcal{N}(0, 1)$. Hence, the statistic for a one-proportion z -test is

$$z = 2\sqrt{m} \left(\frac{T_i}{m} - \frac{1}{2} \right) \quad (3)$$

For a given pair of $(key, value)$ columns, the data-owner can calculate the corresponding z -score by counting the number of elements in *value* column that are in green intervals. Since we are performing multiple hypothesis tests simultaneously if the dataset has 10 pairs of columns and the chosen significant level $\alpha = 0.05$, then the individual threshold for each column is $\alpha_i = 0.0005$. The data-owner can look up the corresponding threshold for the z -score to reject each individual null hypothesis. If the calculated z -score exceeds the threshold, then the data-provider can reject the null hypothesis and claim that this *value* column is watermarked. On the other hand, if the z -score is below the threshold, then the data-owner cannot conclude whether this *value* column is watermarked or not until they have checked all possible *key* columns.

6 Robustness of Pairwise Tabular Data Watermark

In this section, we examine the robustness of the watermarked dataset when they are subjected to different ‘attacks’ commonly seen in data science. We assume that the attacker has no knowledge of the $(key, value)$ pairing scheme and, consequently, has no knowledge of the green intervals. We focus on two types of attacks: feature extraction and truncation, which are common preprocess steps before the dataset can be used for a downstream task.

6.1 Robustness to Feature Selection

Given a watermarked dataset \mathbf{X}_w and a downstream task, a data scientist may want to preprocess the data by dropping irrelevant features from \mathbf{X}_w . Formally, we make the following assumption on how to perform feature selection:

Assumption 6.1. *Given a dataset $\mathbf{X} \in [0, 1]^{m \times 2n}$ with features $\mathbf{X}_1, \dots, \mathbf{X}_{2n}$, the data scientist perform feature selection according to a known feature importance order with regard to the downstream task. Then, the truncated dataset is of size $m \times k$ for $k \leq n$, where only the top- k features with the highest importance are kept from the original dataset.*

Algorithm 1 takes a black-box pairing subroutine PAIR as an input to determine the set of $(key, value)$ columns. In the following analysis, we consider two feature pairing schemes: (i) *uniform*: features are paired uniformly at random, or (ii) *feature importance*: features are paired according to the feature importance ordering, where features with similar importance are paired.

¹With knowledge of the feature importance (detail in Section 6), the data-owner can choose adaptive significant level α for each individual hypothesis test. Informally, we put more weight on pairs of $(key, value)$ columns that are closer together in their feature importance while ensuring that all significant levels sum up to the desired α threshold.

Without loss of generality, we assume that the columns of the original dataset are ordered in descending order of feature importance. Note that this reordering of features does not affect the uniform pairing scheme and only serves to simplify notations in our analysis. Formally, given two columns \mathbf{X}_i and \mathbf{X}_j , we define the probability of $(\mathbf{X}_i, \mathbf{X}_j)$ being a $(key, value)$ pair as proportional to the inverse of the distance between their indices.

$$\Pr[(\mathbf{X}_i, \mathbf{X}_j) \text{ is pair}] = \frac{\frac{1}{|i-j|}}{\sum_{\ell \in [2n], \ell \neq i} \frac{1}{|i-\ell|}} \quad (4)$$

In the following theorem, we show that feature importance pairing will preserve more pairs of columns after the feature selection attack compared to uniform pairing.

Theorem 6.2. *Given a watermarked dataset \mathbf{X}_w and a data scientist attacking \mathbf{X}_w with feature selection as in Assumption 6.1. Then, the number of preserved column pairs under feature importance pairing is at least twice as many as that under uniformly random pairing.*

Theorem 6.2 implies that, under the feature importance pairing scheme, the truncated dataset would retain more valuable information. In Section 8, we empirically show how this theoretical guarantee translates to improved utility in the downstream task for various datasets.

6.2 Robustness to Truncation

In addition to feature selection, the data scientist can also ‘attack’ the watermarked dataset by directly modifying elements in the dataset. In particular, we are interested in ‘truncation’ attack, where the data scientist reduces the number of digits after the decimal point of all elements in the dataset. Formally, let $\text{truncate} : \mathbb{R} \rightarrow \mathbb{R}$ be the truncation function defined as:

$$x_{\text{tr}} = \text{truncate}(x, p) = \frac{\lfloor 10^p \cdot x \rfloor}{10^p} \quad (5)$$

That is, for all $x \in \mathbf{X}_w$, the data scientist truncates the digits in the mantissa of x to $x_{\text{tr}} \in \mathbb{R}$ with p digits in the mantissa. For example, with $x = 0.369$ and $p = 2$, the data scientist will truncate x to get $x_{\text{tr}} = 0.36$. In the following analysis, we focus on the case where $p = 2$, i.e., all values are truncated to 2 decimal places. Extension to more digits in the mantissa follows the same analysis.

First, we determine how this truncation operation influence the distribution of watermarked elements in green intervals. When a watermarked element x in a *value* column is truncated to x_{tr} , it can fall out of the original green interval if the bins $[0, 1/b], \dots, [b-1/b, 1]$ and the hundredth grid points $\{0, 0.01, 0.02, \dots, 0.99, 1\}$ are not perfectly aligned. To illustrate this phenomenon, we presented stylized example where Algorithm 1 uses $b = 150$ bins for its watermarking procedure. Then, in the second bin $I_2 = [1/150, 2/150]$, any element $x \in [1/150, 0.01)$ will be truncated to $x_{\text{tr}} = 0.0 \in I_1$. If I_1 is chosen to be a red interval by the random number generator in Algorithm 1, then the truncation operation has successfully moved elements out of the green intervals. In the following theorem, we show the probability of successful truncation attack as a function of the bin width.

Theorem 6.3. *Given a watermarked element $x \in I_j = [j-1/b, j/b]$ and the truncation function defined in Equation (5). Then, the probability that the truncated element x_{tr} falls out of its original green interval is*

$$\Pr[x_{\text{tr}} \notin I_j] = \frac{(b-1)^{100} + b^{99}(c \cdot b - j + 1)}{b^{100}}$$

where $c \in \{0.00, 0.01, \dots, 1.00\}$ is the left grid point in I_j .

Intuitively, with larger bin size $1/b$, the probability that our proposed watermarking scheme can withstand truncation attack increases as the truncated elements are more likely to fall into the same bins as the original elements. On the other hand, when the bins are more fine-grained, truncation would almost surely move the watermarked data outside of the original intervals. This result presents an interesting trade-off between smaller bin width for higher fidelity (see Theorem 4.1) and bigger bin width for better robustness, which has not been studied in prior work on watermarking tabular data. With this insight, we can choose the bin width to be the same as the truncation grid size, i.e., $1/b = 1/10^p$ or $b = 10^p$ to ensure high fidelity and robustness.

7 Decoding watermark

It is important to understand how many queries are required by an adversary to learn a watermarking scheme. Specifically, this would allow us to bound the total number of queries we can allow one single user before we run the risk of giving out our algorithms. Although such a result has not been studied in prior work [He et al., 2024], we believe it would showcase the power of any watermarking scheme. To this end, we demonstrate that the number of queries an adversary would require to learn the watermarking algorithm presented in our work (Algorithm 1) is $\tilde{O}(mnb)$, where b is the number of bins used to embed the watermark in Algorithm 1, and the adversary uses a query table of size $m \times n$. We informally state this result below, and defer the formal statement and its proof until Appendix E.

Theorem (E.2, Informal). *The watermarking scheme in Algorithm 1 can be learned up to a small error $\epsilon \in (0, 1)$ with probability at least $1 - \delta \in (0, 1)$ by making $O\left(\frac{mnb \log(mnb) \log(1/\epsilon) + \log(1/\delta)}{\epsilon}\right)$ queries to the detector using tables of size $m \times n$.*

In practice, any watermark provider using Algorithm 1 to watermark their data can artificially limit the total number of queries by order or magnitudes less than the query complexity of Theorem E.2 to avoid divulging the watermarking scheme. We also observe that the query complexity of learning Algorithm 1 is exactly same as the query complexity of learning the algorithm of He et al. [2024]. This is an artifact of how we derive our bounds (via VC dimension). Beyond table like queries, we also study the case when queries are of the form of rows. The formal theorem statement and an analysis for the case where queries are of the form of a row can be found in Appendix E.3.

8 Experiments

In this section, we empirically evaluate the fidelity and robustness of our watermarking algorithm on a set of synthetic and real-world datasets.

8.1 Synthetic Tabular Data

We begin our evaluation using synthetic data to validate the properties of our algorithm, including fidelity, robustness, and performance sensitivity to selected parameters.

8.1.1 Experimental Detail

We generate a dataset of size 2000×2 using the standard Gaussian distribution. One column is designated as the seed column, and the other is watermarked. Figures 2a and 2b contain KDE plots showing a minimal difference between the distribution before and after watermarking.

In the second experiment, we generate multiple datasets, each containing 50 columns and varying numbers of rows from 20 to 100, to validate the effect that the row count has on the maximum achievable z -score. We repeat this process 5 times and take the average z -score. In Figure 2c, we find that as the number of rows in the dataset increases, so does the maximum possible z -score. This means that given a choice of z -score threshold, i) there is an increasing minimum number of total rows that the dataset must contain to achieve that score, and ii) as the number of rows increases, so does the number of rows that an attacker must sufficiently alter to break the watermark.

Finally, we consider the *fidelity vs. robustness* trade-off that the *bin size* parameter poses. We generate a dataset of size 2000×2 using the standard Gaussian distribution. We watermark one column, using the other for seeding, and vary the *bin size* between 10^{-4} and 10^{-1} . The average mean squared error across 5 runs between the original data and the watermarked data for each *bin size* is shown in Figure 2d. As expected, greater fidelity is maintained with smaller bins since adjusting the data to fall into the nearest green bin requires smaller perturbations. Figure 2e displays the accompanying susceptibility to noise that comes with smaller bins. Across 5 runs, we add zero-mean Gaussian noise with standard deviation varying from 10^{-3} to 10^{-1} to the watermarked data and measure the effect on the z -score. In each case, we find that smaller bins result in lower scores.

8.1.2 Classification

To validate the effectiveness of our feature importance based pairing scheme, we generate a multi-class classification dataset of size 75×75 using scikit-learn, setting the number of classes to 5 and the number of informative features to 37. We create a set of column pairs using two different schemes: i) *uniform*: features are paired uniformly at random and ii) *feature importance*: sampling columns by treating their feature importance according to a Random Forest classifier as probabilities, pairing columns that are sampled one after the other. Using these two pairing schemes we create two watermarked datasets by watermarking 12 of the 37 available pairs, respectively.

For each of the watermarked datasets, we train a Random Forest classifier and use the resulting feature importance to drop subsets of columns varying in size from 20% to 80%. The metric of interest in this experiment is the percentage of pairs retained after column dropping. Both columns in a pair must still remain in the dataset to be counted as a preserved pair. This entire process is repeated 5 times, and the averaged results are shown in Figure 2f. The results show a significant increase in preserved pairs when the pairs are created using the feature importance scheme.

8.2 Spoofing

We introduce a novel method (Algorithm 2) to spoof and test the robustness of our algorithm by comparing it to the previous work of He et al. [2024]. This spoofing algorithm is designed to subtly alter a dataset by modifying the decimal points of its elements, effectively inserting a watermark to the dataset. The process begins by computing the integers and fractional parts of a synthetic dataset and a reference watermarked dataset. For the experiment shown below Figure 3b, we generated a synthetic dataset of the original unwatermarked dataset to act as our target. For each element in the synthetic dataset, the algorithm identifies the closest fractional part from the watermarked dataset to the current element. If the element is non-negative, the fractional part is added to the integer part. This method ensures that the watermark is embedded in a way that is minimally invasive, preserving the fidelity, detectability, overall structure and

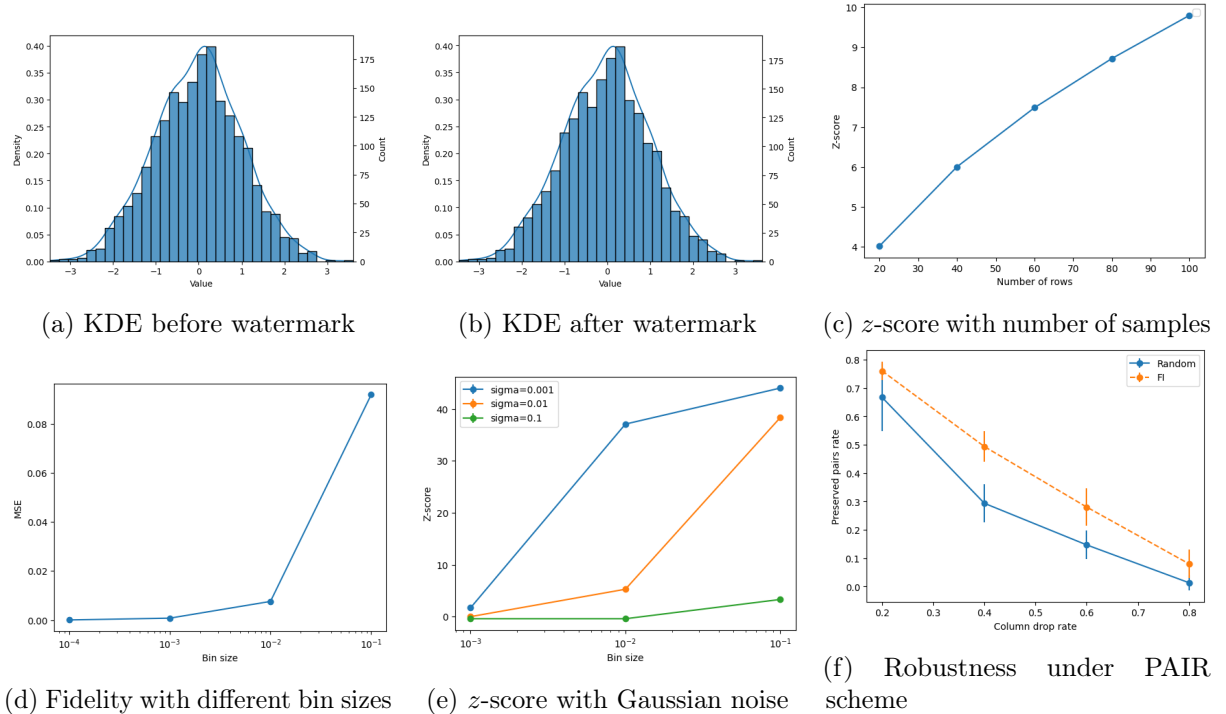


Figure 2: (a) KDE plot of the Gaussian data before watermarking. (b) KDE plot of the Gaussian data after watermarking. (c) The maximum possible z -score increases with the number of rows in the dataset. (d) Smaller bin sizes result in higher fidelity (lower MSE) between the original data and the watermarked data. (e) Smaller bin sizes are more susceptible to noise, resulting in lower z -scores. Sigma corresponds to the standard deviation of the applied zero-mean Gaussian noise. (f) Pairing columns according to feature importance increases the pair preservation rate when the least important features are dropped. ‘Random’ indicates random column pairings while ‘FI’ indicates column pairings biased toward similar feature importances.

integrity of the original data while introducing a subtle, detectable pattern. The experimental results are in Figure 3.

Using Algorithm 2, we can successfully spoof the watermark scheme by prior work [He et al., 2024] after replacing about 40% of the synthetic dataset. That is, the spoofed dataset generated from Algorithm 2 will be classified as ‘watermarked’ by the He et al. [2024]’s detector as the p -value drops below 0.05. On the other hand, our watermark approach (Algorithm 1) cannot be spoofed by using Algorithm 2 at all. Even after all data points in the synthetic dataset have been processed, the p -value from our detection hypothesis test (Section 5) still remains above 0.05. This result shows that our watermark approach is more robust to simple spoofing attack compared to prior work of He et al. [2024] by leveraging the structure of the tabular dataset.

8.3 Generative Tabular Data

In addition to synthetic data, we evaluate the theoretical guarantees of our watermark approach on a set of real-world datasets.

8.3.1 Datasets and Generators

Similar to He et al. [2024], we evaluate our proposed watermarking technique using two real-world datasets of various sizes and distributions: Wilt [Johnson, 2014], and California Housing Prices.

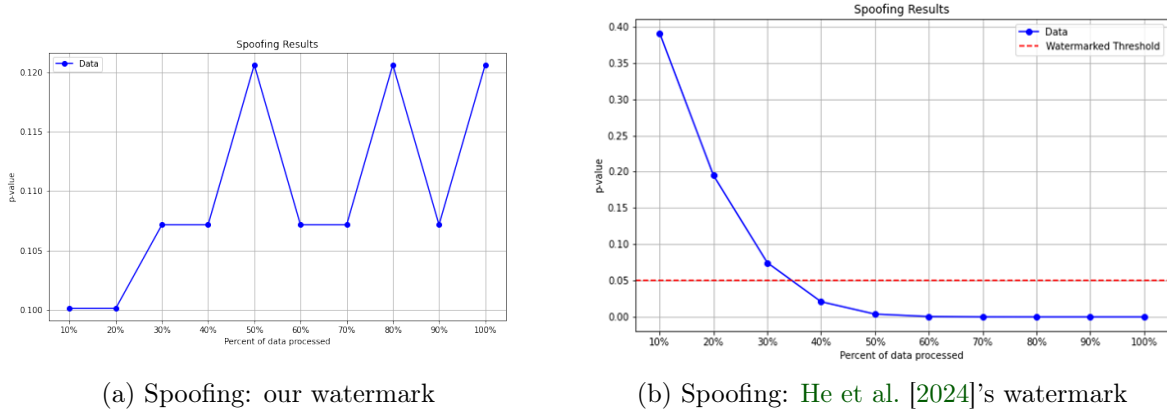


Figure 3: (a) Plot of our replacement spoofing algorithm on our watermark approach. Our approach is highly robust as the spoofing algorithm as well as the percent of data processed has no effect on our dataset. (b) Plot of our replacement spoofing algorithm on He et al. [2024]’s watermark approach. As the percentage of data processed increases, the p -value decreases. As the percent of data processed increases near 40%, the p -value of He et al. [2024]’s watermark is already below 0.05 and the watermark can be spoofed using Algorithm 2.

Wilt. This dataset is a public dataset that is part of the UCI Machine Learning Repository. It contains data from a remote sensing study that involved detecting diseased trees in satellite imagery. The data set consists of image segments generated by segmenting the pan-sharpened image. The segments contain spectral information from the Quickbird multispectral image bands and texture information from the panchromatic (Pan) image band². This dataset includes 4,889 records and 6 attributes. The attributes are a mixture of numerical and categorical data types. The data set has a binary target label, which indicates whether a tree is wilted or healthy. Therefore, the dataset has a classification task, which is to classify the tree samples as either diseased or healthy.

California Housing Prices. The dataset was collected from the 1990 U.S. Census and includes various socio-economic and geographical features that are believed to influence housing prices in a given California district. It contains 20,640 records and 10 attributes, each of which represents data about homes in the district. Similar to the previous dataset, the attributes are a mixture of continuous and categorical data types. The dataset has a multi-target label, which indicates the proximity of each house to the ocean, making it a multi-classification problem.

For each dataset, we generate corresponding synthetic datasets using neural network-based methods Park et al. [2018] and statistical-based generative methods Li et al. [2020]. Each of these methods for synthetic data generation possesses distinctive capabilities and features. For this paper, we employ CTGAN [Xu et al., 2019], Gaussian Copula [Masarotto and Varin, 2012], and TVAE [Xu et al., 2019] which represent GAN-based [Goodfellow et al., 2014], copula-based [Patki et al., 2016], and VAE-based generators [Kingma and Welling, 2013] respectively to generate tabular data.

8.3.2 Utility

For evaluating utility, we focus on machine learning (ML) efficiency [Xu et al., 2019]. In more detail, ML efficiency quantifies the performance of classification or regression models that are

²Data available on the UCI platform at <https://archive.ics.uci.edu/dataset/285/wilt>

Algorithm 2: Fractional Replacement

Input: Synthetic dataset $\mathbf{S} \in \mathbb{R}^{m \times n}$, Watermarked dataset $\mathbf{W} \in \mathbb{R}^{m \times n}$.

Output: Modified dataset \mathbf{X}' .

- 1: Compute the fractional parts of \mathbf{S} to form $\mathbf{S_fractions}$.
- 2: Compute the fractional parts of \mathbf{W} to form $\mathbf{W_fractions}$.
- 3: **for** each element x_{ij} in \mathbf{S} **do**
- 4: Extract the integer part $\lfloor x_{ij} \rfloor$.
- 5: Compute the fractional part $\text{frac_part} = |x_{ij} - \lfloor x_{ij} \rfloor|$.
- 6: Find the closest fractional part
 $\text{closest_frac} = \arg \min_{f \in \mathbf{S_fractions} \cup \mathbf{W_fractions}} |f - \text{frac_part}|$.
- 7: **if** $x_{ij} < 0$ **then**
- 8: Replace x_{ij} with $\lfloor x_{ij} \rfloor - \text{closest_frac}$.
- 9: **else**
- 10: Replace x_{ij} with $\lfloor x_{ij} \rfloor + \text{closest_frac}$.

Dataset	Method	Not WM	Watermarked (WM)					
			WM	WM and Truncated	WM and 20% cols drop		WM and 40% cols drop	
					FI	Random	FI	Random
California	CTGAN	0.373	0.371	0.368	0.301	0.242	0.203	0.256
	Copula	0.370	0.376	0.376	0.347	0.332	0.31	0.30
	TVAE	0.797	0.799	0.798	0.448	0.407	0.385	0.365
Wilt	CTGAN	0.731	0.733	0.733	0.575	0.574	0.563	0.563
	Copula	0.99	0.996	0.996	0.995	0.994	0.993	0.993
	TVAE	0.989	0.989	0.989	0.965	0.977	0.972	0.803

Table 2: Accuracy of the downstream models under various attacks to the watermarked datasets. In particular, we provide accuracy for the original dataset and its watermarked counterpart. Additionally, we consider truncation as well as the column dropping separately that are typical preprocessing steps in a machine learning pipeline. We note that the effect of our watermarking technique is negligible in terms of accuracy in all cases while maintaining high detectability.

trained on synthetic data and evaluated on the real test set. In our experiment, we evaluate ML efficiency with respect to the XGBoost classifier [Chen and Guestrin, 2016] for classification tasks, which are then evaluated on real testing sets. Classification performances are evaluated by the accuracy score. To explore the performance of our tabular watermark on real-world data, we sample from each generative model a generated dataset with the size of a real training set. For each setup, we create 5 watermarked training sets to measure the accuracy score. For reproducibility, we set a specific random seed to ensure that the data deformation and model training effects are repeatable on a similar hardware and software stack. To eliminate the randomness of the results, the experimental outcomes are averaged over multiple runs from each watermarked training set.

We watermark each of the generated datasets using a *bin size* of 10^{-2} and thus only consider columns that contain floating point numbers with at least 2 decimal places. This choice follows from the practical consideration that watermarking with this bin size involves perturbing up to 2 decimal places, and watermarking any original columns that did not already contain values with this property may make it obvious to an outside party upon receiving the dataset that this specific section of the data has been manipulated.

We also consider two common data science preprocessing steps that downstream users of the watermarked datasets might conduct: truncation and dropping the least important columns. We aim to determine if the application of our watermark in conjunction with these operations For the former, we truncate to 2 decimal places. For the latter, we investigate dropping the lowest 20% and 40% of columns in each case, considering when the data is watermarked both with and without the feature importance-based pairing scheme.

We find that the effect of our watermarking technique is negligible in terms of accuracy in all cases while maintaining high detectability as seen in Table 2.

9 Discussion and Future Work

In this work, we provided a novel robust watermarking scheme for tabular numerical datasets. Our watermarking method partitions the feature space into pairs of $(key, value)$ columns using knowledge of the feature importance in the downstream task. We use the center of the bins from each *key* columns to generate randomized red and green intervals and watermark the *value* columns by promoting its value to fall in green intervals. Compared to prior work in watermarking generative tabular data, our method is more robust to preprocess attacks such as feature selection and truncation at the cost of harder detection. There are a few open questions in the current work that are ripe for investigation:

- How do we include the categorical columns either in the key or the value of the watermarking process? Note that in the LLM setting, this was possible due to the richness of the vocabulary, which enabled replacing one token with a close enough token with a similar semantic meaning.
- Can we extend this framework to the LLM settings for tabular data generation? This extension embeds the watermark as part of the generation process [Venugopal et al., 2011] and the results in this paper will need to be adapted to the new setting. The samples generated by the LLM will be distorted due to the additional watermarking step, and recent work [Kuditipudi et al., 2024] mitigates it by inducing correlations with secret keys. A similar injection of undetectable watermarks has been studied by Christ et al. [2023]. Adapting these to our settings would be of great interest.
- The current watermark scheme only considers a ‘hard’ watermark, where all elements in the *value* columns are deterministically placed in the nearest green intervals. Can we extend the current analysis to allow for a ‘soft’ watermark scheme similar to the one described in Kirchenbauer et al. [2023], where we first promote the probability of being in green intervals, then sample from such distribution to generate elements for the *value* columns?
- Our bounds for the query complexity to decode the query algorithm uses a specific embedding that allows us to apply VC dimensional bounds for learning the query function using neural networks with piecewise linear polynomial functions. It remains open whether one can derive a better query complexity bounds for learning the query function without resorting only to neural networks.

Disclaimer. This paper was prepared for informational purposes by the Artificial Intelligence Research group and the Global Technology Applied Research center of JPMorgan Chase & Co. and its affiliates (“JP Morgan”) and is not a product of the Research Department of JP Morgan. JP Morgan makes no representation and warranty whatsoever and disclaims all liability, for the completeness, accuracy or reliability of the information contained herein. This document is not

intended as investment research or investment advice, or a recommendation, offer or solicitation for the purchase or sale of any security, financial instrument, financial product or service, or to be used in any way for evaluating the merits of participating in any transaction, and shall not constitute a solicitation under any jurisdiction or to any person, if such solicitation under such jurisdiction or to such person would be unlawful.

References

S. Aaronson. ‘Reform’ AI Alignment with Scott Aaronson. AXRP - the AI X-risk Research Podcast, 2023. URL <https://axrp.net/episode/2023/04/11/episode-20-reform-ai-alignment-scott-aaronson.html>.

R. Agrawal and J. Kiernan. Watermarking relational databases. In *VLDB’02: Proceedings of the 28th International Conference on Very Large Databases*, pages 155–166. Elsevier, 2002.

B. An, M. Ding, T. Rabbani, A. Agrawal, Y. Xu, C. Deng, S. Zhu, A. Mohamed, Y. Wen, T. Goldstein, et al. Benchmarking the robustness of image watermarks. *arXiv preprint arXiv:2401.08573*, 2024.

S. A. Assefa, D. Dervovic, M. Mahfouz, R. E. Tillman, P. Reddy, and M. Veloso. Generating synthetic data in finance: opportunities, challenges and pitfalls. In *Proceedings of the First ACM International Conference on AI in Finance*, pages 1–8, 2020.

M. J. Atallah, V. Raskin, M. Crogan, C. Hempelmann, F. Kerschbaum, D. Mohamed, and S. Naik. Natural language watermarking: Design, analysis, and a proof-of-concept implementation. In *Information Hiding: 4th International Workshop, IH 2001 Pittsburgh, PA, USA, April 25–27, 2001 Proceedings 4*, pages 185–200. Springer, 2001.

P. L. Bartlett, N. Harvey, C. Liaw, and A. Mehrabian. Nearly-tight vc-dimension and pseudodimension bounds for piecewise linear neural networks. *Journal of Machine Learning Research*, 20(63):1–17, 2019.

C. Bonferroni. Teoria statistica delle classi e calcolo delle probabilita. *Pubblicazioni del R istituto superiore di scienze economiche e commerciali di firenze*, 8:3–62, 1936.

T. Chen and C. Guestrin. Xgboost: A scalable tree boosting system. In *Proceedings of the 22nd ACM SIGKDD international conference on knowledge discovery and data mining*, pages 785–794, 2016.

M. Christ, S. Gunn, and O. Zamir. Undetectable watermarks for language models. *arXiv preprint arXiv:2306.09194*, 2023.

V. Chvátal. Mastermind. *Combinatorica*, 3:325–329, 1983. doi: 10.1007/BF02579188. URL <https://doi.org/10.1007/BF02579188>.

A. Gonzales, G. Guruswamy, and S. R. Smith. Synthetic data in health care: A narrative review. *PLOS Digital Health*, 2(1):e0000082, 2023.

I. Goodfellow, J. Pouget-Abadie, M. Mirza, B. Xu, D. Warde-Farley, S. Ozair, A. Courville, and Y. Bengio. Generative adversarial nets. *Advances in neural information processing systems*, 27, 2014.

A. Hamadou, X. Sun, S. A. Shah, and L. Gao. A weight-based semi-fragile watermarking scheme for integrity verification of relational data. *International Journal of Digital Content Technology and Its Applications*, 5:148–157, 2011. URL <https://api.semanticscholar.org/CorpusID:58278938>.

H. He, P. Yu, J. Ren, Y. N. Wu, and G. Cheng. Watermarking generative tabular data, 2024. URL <https://arxiv.org/abs/2405.14018>.

B. Johnson. Wilt. UCI Machine Learning Repository, 2014. DOI: <https://doi.org/10.24432/C5KS4M>.

J. Jordon, L. Szpruch, F. Houssiau, M. Bottarelli, G. Cherubin, C. Maple, S. N. Cohen, and A. Weller. Synthetic data-what, why and how? *arXiv preprint arXiv:2205.03257*, 2022.

N. S. Kamaruddin, A. Kamsin, L. Y. Por, and H. Rahman. A review of text watermarking: theory, methods, and applications. *IEEE Access*, 2018.

S. Katzenbeisser and F. Petitcolas. Digital watermarking. *Artech House, London*, 2:2, 2000.

D. P. Kingma and M. Welling. Auto-encoding variational bayes. *arXiv preprint arXiv:1312.6114*, 2013.

J. Kirchenbauer, J. Geiping, Y. Wen, J. Katz, I. Miers, and T. Goldstein. A watermark for large language models. *arXiv preprint arXiv:2301.10226*, 2023.

D. E. Knuth. The computer as master mind. *Journal of Recreational Mathematics*, 9(1):1–6, 1976.

R. Kuditipudi, J. Thickstun, T. Hashimoto, and P. Liang. Robust distortion-free watermarks for language models. *Transactions on Machine Learning Research*, 2024. ISSN 2835-8856. URL <https://openreview.net/forum?id=FpaCL1MO2C>.

Z. Li, Y. Zhao, and J. Fu. Sync: A copula based framework for generating synthetic data from aggregated sources. In *2020 International Conference on Data Mining Workshops (ICDMW)*, pages 571–578. IEEE, 2020.

G. Masarotto and C. Varin. Gaussian copula marginal regression. *Electronic Journal of Statistics*, 6:1517–1549, 2012. URL <https://api.semanticscholar.org/CorpusID:53962593>.

N. Park, M. Mohammadi, K. Gorde, S. Jajodia, H. Park, and Y. Kim. Data synthesis based on generative adversarial networks. *arXiv preprint arXiv:1806.03384*, 2018.

N. Patki, R. Wedge, and K. Veeramachaneni. The synthetic data vault. In *2016 IEEE international conference on data science and advanced analytics (DSAA)*, pages 399–410. IEEE, 2016.

V. K. Potluru, D. Borrajo, A. Coletta, N. Dalmasso, Y. El-Laham, E. Fons, M. Ghassemi, S. Gopalakrishnan, V. Gosai, E. Kreačić, et al. Synthetic data applications in finance. *arXiv preprint arXiv:2401.00081*, 2023.

S. Shalev-Shwartz and S. Ben-David. *Understanding machine learning: From theory to algorithms*. Cambridge university press, 2014.

M. Shehab, E. Bertino, and A. Ghafoor. Watermarking relational databases using optimization-based techniques. *IEEE transactions on Knowledge and Data Engineering*, 20(1):116–129, 2007.

R. Sion, M. Atallah, and S. Prabhakar. Rights protection for relational data. In *Proceedings of the 2003 ACM SIGMOD International Conference on Management of Data*, SIGMOD '03, page 98–109, New York, NY, USA, 2003. Association for Computing Machinery. ISBN 158113634X. doi: 10.1145/872757.872772. URL <https://doi.org/10.1145/872757.872772>.

A. Venugopal, J. Uszkoreit, D. Talbot, F. J. Och, and J. Ganitkevitch. Watermarking the outputs of structured prediction with an application in statistical machine translation. In *Proceedings of Empirical Methods for Natural Language Processing*, 2011.

X. Xiao, X. Sun, and M. Chen. Second-lsb-dependent robust watermarking for relational database. In *Third International Symposium on Information Assurance and Security*, pages 292–300, 2007. doi: 10.1109/IAS.2007.25.

L. Xu, M. Skoularidou, A. Cuesta-Infante, and K. Veeramachaneni. Modeling tabular data using conditional gan. *Advances in neural information processing systems*, 32, 2019.

Y. Zheng, H. Xia, J. Pang, J. Liu, K. Ren, L. Chu, Y. Cao, and L. Xiong. Tabularmark: Watermarking tabular datasets for machine learning, 2024. URL <https://arxiv.org/abs/2406.14841>.

A Proof of Fidelity

Proofs of Theorem 4.1

Proof. Observe that the watermarked dataset \mathbf{X}_w only differs from the original dataset \mathbf{X} in the *value* columns. For each element x in the *value* column of the original dataset \mathbf{X} , let Y denote the chosen nearest interval from the green list. Then, we have

$$\begin{aligned}
& \mathbb{E}[|x - x_w|] \\
& \leq \max_{y \in Y} \mathbb{E}[|x - y|] \\
& \leq \max_{y \in Y} \mathbb{E} \left[|x - y| \mid |x - y| \leq \frac{k}{b} \right] \cdot \Pr \left[|x - y| \leq \frac{k}{b} \right] \\
& \quad + \mathbb{E} \left[|x - y| \mid |x - y| > \frac{k}{b} \right] \cdot \Pr \left[|x - y| > \frac{k}{b} \right] \\
& \leq \max_{y \in Y} \frac{k}{b} \cdot \left(1 - \frac{1}{2^k} \right) + 1 \cdot \frac{1}{2^k} \\
& = \frac{k(2^k - 1)}{b \cdot 2^k} + \frac{1}{2^k} \\
& = \frac{k \cdot (2^k - 1) + 2b}{b \cdot 2^k}
\end{aligned}$$

where $k \in [1, b]$ is a variable denoting the search radius for the nearest green interval. Then, choosing $\delta = \frac{1}{2^k}$ and taking union bound over all elements, we have with probability at least $1 - \delta$:

$$\mathbb{E}[\|\mathbf{X} - \mathbf{X}_w\|_\infty] \leq \frac{\log_2(mn/\delta)}{b}$$

□

Proof of Corollary 4.2

Proof. By definition of k -Wasserstein distance, we have with probability at least $1 - \delta$ for $\delta \in (0, 1)$:

$$\begin{aligned}
& \mathcal{W}_k(F_{\mathbf{X}}, F_{\mathbf{X}_w}) \\
& \leq \left(\sum_{j=1}^m \frac{1}{m} \|\mathbf{X}[j, :] - \mathbf{X}_w[j, :]\|_2^k \right)^{1/k} \\
& \leq \left(\sum_{j=1}^m \frac{1}{m} \left(\sqrt{2n} \|\mathbf{X}[j, :] - \mathbf{X}_w[j, :]\|_{\infty} \right)^k \right)^{1/k} \\
& \leq \left(\sum_{j=1}^m \frac{1}{m} \left(\sqrt{2n} \cdot \frac{\log_2(mn/\delta)}{b} \right)^k \right)^{1/k} \\
& = \left(\sum_{j=1}^m \frac{1}{m} \frac{(\sqrt{2n} \cdot \log_2(mn/\delta))^k}{b^k} \right)^{1/k} \\
& = \frac{\sqrt{2n} \cdot \log_2(mn/\delta)}{b}
\end{aligned}$$

□

B Proofs of Detectability

Proof of Lemma 5.1

Proof. Let $I_j = \left[\frac{j-1}{b}, \frac{j}{b} \right]$ denote an interval on $[0, 1]$. Then, for each element x in a *value* column, we have:

$$\begin{aligned}
\Pr_{x \sim F}[x \in G] &= \Pr_{x \sim F}\left[\bigcup_{j=1}^b \{x \in I_j \& I_j \in G\}\right] \\
&= \sum_{j=1}^b \Pr_{x \sim F}[x \in I_j \& I_j \in G] \\
&= \sum_{j=1}^b \Pr[x \in I_j | I_j \in G] \cdot \Pr[I_j \in G] \\
&= \sum_{j=1}^b \Pr[x \in I_j] \cdot \frac{1}{2} \\
&= \frac{1}{2}
\end{aligned}$$

□

C Proofs of Robustness

Proof of Theorem 6.2

Proof. We first look at the number of preserved columns under uniform pairing.

Uniform pairing. Let $\mathbf{X}'_w \in [0, 1]^{m \times k}$ denote the watermarked dataset after feature selection.

Consider the set of all possible pairs of columns after feature selection can be matched together. Then, there are $\binom{k}{2}$ possible choices, which are the number of 2-subset from k total columns. Define an event $Y_\ell = \mathbf{1}[\ell\text{-th subset is a pair}]$. In each 2-subset, after a first column is selected, the probability that the second column actually forms a pair with the first column is $1/2n-1$. Hence, we have:

$$\mathbb{E}[Y_\ell] = \frac{1}{2n-1}$$

Hence, the expected number of preserved pairs of columns in \mathbf{X}'_w under uniform random pairing can be obtained by summing over all $\binom{k}{2}$ possible choices as follow.

$$\begin{aligned} \mathbb{E}[\text{number of preserved pairs } \in \mathbf{X}'_w] &= \sum_{\ell=1}^{\binom{k}{2}} \mathbb{E}[Y_\ell] \\ &= \binom{k}{2} \frac{1}{2n-1} \\ &= \frac{(k-1)k}{2(2n-1)} \end{aligned}$$

Now, we can look at the number of preserved pairs of columns under feature importance pairing. Note that we assume the feature selection is performed according to Assumption 6.1, and the columns are in descending order of feature importance. Since we are only retaining the top k most important features after feature selection, this is equivalent to counting the number of preserved pairs among the first k features after reordering.

Feature importance pairing. When the columns are paired according to the feature importance ordering, we match them according to Equation (4). Define the event $Y_{i,j} = \mathbf{1}[\text{columns } (i, j) \text{ is a pair}]$. Then, for fixed columns i and j , we have:

$$\begin{aligned} \mathbb{E}[Y_\ell] &= \frac{\frac{1}{|i-j|}}{\sum_{j \neq i}^{2n} \frac{1}{|i-j|}} \\ &= \frac{\frac{1}{|i-j|}}{\sum_{\ell=1}^{i-1} \frac{1}{\ell} + \sum_{s=1}^{2n-i} \frac{1}{s}} \\ &= \frac{\frac{1}{|i-j|}}{H_{i-1} + H_{2n-i}} \end{aligned}$$

where H_i is the i -th harmonic number. We know that for $i \geq 1$, we have $\ln(i+1) \leq H_i \leq \ln(i) + 1$. Let $\Delta_i = \max\{i-1, 2n-i\}$. Since only the top- k columns are retained, we have:

$$\begin{aligned} \mathbb{E}[\text{number of preserved pairs } \in \mathbf{X}'_w] &= \sum_{i=1}^k \sum_{j \neq i, j=1}^k \frac{1}{|i-j| (H_{i-1} + H_{2n-i})} \\ &= \sum_{i=1}^k \frac{1}{H_{i-1} + H_{2n-i}} \left(\sum_{j \neq i, j=1}^k \frac{1}{|i-j|} \right) \end{aligned}$$

$$\begin{aligned}
&= \sum_{i=1}^k \frac{1}{H_{i-1} + H_{2n-i}} (H_{i-1} + H_{k-i}) \\
&= \sum_{i=1}^k 1 - \frac{H_{2n-i} - H_{k-i}}{H_{i-1} + H_{2n-i}} \\
&= k - \sum_{i=1}^k \frac{H_{2n-i} - H_{k-i}}{H_{i-1} + H_{2n-i}} \\
&\geq k - \sum_{i=1}^k \frac{H_{2n-i}}{H_{i-1} + H_{2n-i}}
\end{aligned}$$

Since we assume that $k < n$, we have

$$\begin{aligned}
i < n &\Rightarrow 2n - i > n > i - 1 \\
&\Rightarrow \frac{1}{i-1} > \frac{1}{2n-i} \\
&\Rightarrow H_{i-1} < H_{2n-i} \\
&\Rightarrow \frac{H_{2n-i}}{H_{i-1} + H_{2n-i}} > \frac{1}{2}
\end{aligned}$$

Therefore, the expected number of preserved pairs under feature importance pairing is $k/2$.

Finally, we can compare the number of preserved pairs under the two pairing schemes:

$$\begin{aligned}
\frac{\frac{k}{2}}{\frac{(k-1)k}{2(2n-1)}} &= \frac{k}{2} \frac{2(2n-1)}{(k-1)k} \\
&= \frac{2n-1}{k-1} \\
&\geq \frac{2k-1}{k-1} \\
&> \frac{2k-2}{k-1} \\
&= 2
\end{aligned}$$

Therefore, we retain twice as many pairs of $(key, value)$ columns by using feature importance pairing scheme compared to the naive approach of uniformly random pairing. \square

Proof of Theorem 6.3

Proof. If x_{tr} falls out of the original green interval I_j , then we know that either $x_{\text{tr}} > j/b$ or $x_{\text{tr}} < j-1/b$. Since $b \leq 10^p$, we know that the green interval I_j lies in the union of at most two consecutive grids. We consider two cases depending on whether I_j contains a grid point or not.

When I_j does not contain a grid point. Since the truncation function defined in Equation (5) always truncate an element x to the nearest left grid point, which lies outside of I_j , we have

$$\Pr [x_{\text{tr}} \notin I_j | c \notin I_j, \forall c \in \text{grid}] = 1.$$

When I_j contains a grid point. Let c denote the grid point in I_j . Then, when the interval I_j contains a grid point, we have:

$$\begin{aligned}\Pr[x_{\text{tr}} \notin I_j | c \in I_j] &= \Pr\left[x \in \left[\frac{j-1}{b}, c\right)\right] \\ &= \frac{c - \frac{j-1}{b}}{\frac{1}{b}} \\ &= c \cdot b - j + 1\end{aligned}$$

Then, summing over all possible events, we have the probability that the truncation attack successfully moves a watermarked element out of its original green interval is:

$$\begin{aligned}\Pr[x_{\text{tr}} \notin I_j] &= \Pr[x_{\text{tr}} \notin I_j | c \notin I_j, \forall c \in \text{grid}] \cdot \Pr[c \notin I_j, \forall i \in \text{grid}] \\ &\quad + \Pr[x_{\text{tr}} \notin I_j | c \in I_j] \cdot \Pr[c \in I_j] \\ &= \Pr[c \notin I_j, \forall c \in \text{grid}] + (c \cdot b - j + 1) \Pr[c \in I_j] \\ &= \left(\frac{b-1}{b}\right)^{10^p} + \frac{c \cdot b - j + 1}{b} \\ &= \frac{(b-1)^{10^p} + b^{10^p-1}(c \cdot b - j + 1)}{b^{10^p}}\end{aligned}$$

Hence, the probability that x_{tr} is in a red interval is $\rho_{\text{trunc}} = \frac{(b-1)^{10^p} + b^{10^p-1}(c \cdot b - j + 1)}{2b^{10^p}}$.

Let $n_\alpha = \alpha \sqrt{\frac{m}{4}} + \frac{m}{2}$ be the minimum number of cells in the green intervals for the z -score to be at least α . For the watermark to be removed, the attacker needs to truncate at least $m - n_\alpha$ cells in a column. Therefore, the expected number of attacked cells is $\frac{m - n_\alpha}{\rho_{\text{trunc}}}$. \square

C.1 Robustness to additive noise

Theorem C.1. Fix a column in the watermarked dataset. Let n_a be the number of cells in this column that an adversary can inject noise into. If the noise injected into each cell is drawn i.i.d from an uniform distribution, i.e., $\epsilon \sim \text{Unif}[-\sigma, \sigma]$, then the expected number of cells needed to remove the watermark is:

$$\mathbb{E}[n_a] = \frac{m - n_\alpha}{\rho}$$

where $n_\alpha = \alpha \sqrt{\frac{m}{4}} + \frac{m}{2}$ is the minimum number of cells in the green intervals for the z -score to be at least α , and $\rho = 0.5 - \frac{1}{4b\sigma}$.

Proof. Consider a green cell x , where $x \in I_j = [j-1/b, j/b]$. When x is attacked with additional noise ϵ , the modified cell $x + \epsilon$ is no longer in the original green interval is $\Pr[x + \epsilon > j/b] + \Pr[x + \epsilon < j-1/b]$. Formally, we have:

$$\begin{aligned}\Pr[x + \epsilon \notin I_j] &= \Pr\left[x + \epsilon > \frac{j}{b}\right] + \Pr\left[x + \epsilon < \frac{j-1}{b}\right] \\ &= \frac{1 - \frac{j}{b} - x + \sigma}{2\sigma} + \frac{\frac{j-1}{b} - x + \sigma}{2\sigma} \\ &= 1 - \frac{1}{2b\sigma}\end{aligned}$$

Hence, the probability that $x + \epsilon$ is in a red interval is $0.5 - \frac{1}{4b\sigma}$.

For the watermark to be removed, the attacker needs to inject noise into at least $m - n_\alpha$ cells of the columns. Therefore, the expected number of attacked cells is $\frac{m - n_\alpha}{0.5 - \frac{1}{4b\sigma}}$. \square

D Additional experimental details

For synthetic data generation using three generative methods mentioned in the paper, we follow the default hyperparameters found in the SDV library [Patki et al., 2016]. We run the experiments on a machine type of g4dn.4xlarge consisting of 16 CPU, 64GB RAM, and 1 GPU. For Utility evaluation, default parameters of the XGBoost classifier [Chen and Guestrin, 2016] and Random Forest classifier with a seed of 42 was used. The synthetic data generation, training and evaluation process typically finishes within 4 hours. Python 3.8 version was used to run the experiments.

D.1 Standard deviation

To investigate the performance of our tabular watermark on real-world data, we sample from each generative model a generated dataset. For each setup, we create 5 watermarked training sets of each generator so as to measure the mean accuracy and standard deviation. We use XGBoost classifier and Random Forest classifier for classification tasks which are then evaluated on real testing sets.

Dataset	Method	Not WM	Watermarked (WM)			
			WM	WM and Truncated	WM and 40% cols drop	
					FI	Random
California	CTGAN	0.373 ± 0.02	0.371 ± 0.01	0.368 ± 0.01	0.203 ± 0.1	0.256 ± 0.05
	Copula	0.371 ± 0.02	0.376 ± 0.03	0.376 ± 0.03	0.31 ± 0.1	0.30 ± 0.13
	TVAE	0.797 ± 0.02	0.799 ± 0.02	0.798 ± 0.02	0.385 ± 0.19	0.365 ± 0.08
Wilt	CTGAN	0.731 ± 0.03	0.733 ± 0.04	0.733 ± 0.04	0.563 ± 0.03	0.563 ± 0.03
	Copula	0.99 ± 0.01	0.996 ± 0.01	0.996 ± 0.01	0.993 ± 0.02	0.993 ± 0.02
	TVAE	0.989 ± 0.00	0.989 ± 0.00	0.989 ± 0.00	0.972 ± 0.04	0.803 ± 0.01

Table 3: Accuracy of the downstream models under various attacks to the watermarked datasets. In particular, we provide accuracy for the original dataset and its watermarked counterpart. Classifier used for utility evaluation is **XGBoost**. In addition to this, we add the standard deviation of each record.

D.2 Detection computation

We further investigate the effects that algorithm parameters and downstream manipulations have on the robustness and computational requirements of the detection mechanism. We measure the number of column pairing tests that must be done before a high confidence pair is found. We define high confidence as achieving a z -score of 4 using 24 randomly selected rows. The process is stopped early when the watermark is detected. Thus, when a watermark cannot be found, the result becomes $N^2 - N$, where N is the number of columns in the dataset.

We compare non-watermarked and watermarked data, and also test with truncation and dropped columns as before. For the latter, here, we compare the 4 total combinations of column ordering choices: watermarking and detection both present the option to order by feature

Dataset	Method	Not WM	Watermarked (WM)			
			WM	WM and Truncated	WM and 40% cols drop	
					FI	Random
California	CTGAN	0.379 ± 0.01	0.379 ± 0.01	0.382 ± 0.01	0.309 ± 0.13	0.334 ± 0.12
	Copula	0.377 ± 0.02	0.393 ± 0.03	0.393 ± 0.03	0.278 ± 0.18	0.333 ± 0.07
	TVAE	0.805 ± 0.02	0.809 ± 0.02	0.808 ± 0.02	0.399 ± 0.19	0.449 ± 0.18
Wilt	CTGAN	0.849 ± 0.04	0.856 ± 0.04	0.859 ± 0.04	0.644 ± 0.40	0.617 ± 0.42
	Copula	0.986 ± 0.01	0.986 ± 0.01	0.985 ± 0.01	0.973 ± 0.02	0.969 ± 0.02
	TVAE	0.985 ± 0.00	0.985 ± 0.00	0.985 ± 0.00	0.985 ± 0.00	0.81 ± 0.40

Table 4: Accuracy of the downstream models under various attacks to the watermarked datasets. In particular, we provide accuracy for the original dataset and its watermarked counterpart. Classifier used for utility evaluation is **Random Forest**. In addition to this, we add the standard deviation of each record.

Dataset	Method	Not watermarked	Watermarked	Watermarked & truncated
California	CTGAN	72 ± 0	16 ± 0	19.6 ± 4.41
	Copula	72 ± 0	16 ± 0	30 ± 4.94
	TVAE	72 ± 0	58.6 ± 11.11	58.4 ± 11.35
Wilt	CTGAN	20 ± 0	9.2 ± 4.62	9.2 ± 4.62
	Copula	20 ± 0	5.4 ± 3.5	5.6 ± 3.38
	TVAE	20 ± 0	2.4 ± 0.5	2.2 ± 0.4

Table 5: Number of column pair tests executed during detection process. The process is stopped early when the watermark is detected. Thus, when a watermark cannot be found, the result becomes $N^2 - N$, where N is the number of columns in the dataset.

importance or to order randomly. We find that, with truncation, it generally takes the same number of computations as without, and that this amount is significantly lower than the upper bound in the ‘Not watermarked’ column.

E Decoding algorithms

Consider the case that the continuous space in $(0, 1]$ is uniformly discretized using bins of size $1/b$ i.e., construct bins in $(0, 1]$ as $-\{(0, \frac{1}{b}], (\frac{1}{b}, \frac{2}{b}], \dots, (\frac{b-1}{b}, 1]\}$. Then each of these bins are labeled $\{0, 1\}$ with some probability $1 - p_i$ and p_i respectively. We save this data-structure. During query time, each entry of the input table/row is checked to see if the values fall into the bins labeled 1. One can then compute z -scores based on the count of watermarked data identified in the input table. The output of the query function is $\{0, 1\}$ if the table is not watermarked or watermarked, respectively.

For a given input to the query function and the output watermark label, we formalize this problem as a learning problem as follows.

Assumptions. We assume that the number of bins b is known to the detection algorithm. We make such an assumption because we use a statistical learning algorithm for detection, and if b is not known apriori, the VC dimension of the relevant hypothesis class becomes infinity, giving us vacuous sample complexity bounds. The algorithm generating the watermark fixes a probability $p \in (0, 1)$, which is hidden from the detection algorithm. The watermarking algorithm draws b

independent and identically distributed samples from the Bernoulli distribution with parameter p . Let $y_1, \dots, y_b \in \{0, 1\}$ denote the observed values. For $k \in [b]$, we interpret y_k to be the label of the interval (or bin) $(\frac{k-1}{b}, \frac{k}{b}]$.

Query function. Let $\Pi: (0, 1] \rightarrow [b]$ denote the canonical projection onto the bins, defined as $\Pi(x) = k$ if $x \in (\frac{k-1}{b}, \frac{k}{b}]$ for $k \in [b]$. Clearly, Π determines the index of the bin into which the input falls. Given a tabular data $\mathbf{X} \in (0, 1]^{m \times n}$ as input, we denote $\Pi^{m \times n}: (0, 1]^{m \times n} \rightarrow [b]^{m \times n}$ to be the function that implements Π entry wise on \mathbf{X} . Let $F_z: [b]^{m \times n} \rightarrow \mathbb{R}$ be a z -score function (chosen based on the problem), which first maps the index of the bin in each entry of the tabular data to the corresponding label of that bin, and then processes these labels in an appropriate fashion.

We define the *query function* $Q: (0, 1]^{m \times n} \rightarrow \{0, 1\}$ given by $Q(\mathbf{x}) = \text{sgn}(F_z(\Pi^{m \times n}(\mathbf{x})))$, where $\text{sgn}: \mathbb{R} \rightarrow \{0, 1\}$ is the sign (or indicator) function defined as

$$\text{sgn}(x) = \begin{cases} 1 & \text{if } x > 0 \\ 0 & \text{otherwise.} \end{cases} \quad (6)$$

The query function tells us whether (1) or not (0) the input data is watermarked. Since the labels y_k are not known to the detection algorithm, the query function is also not known.

Goal. We want to approximate the query function up to a small prediction error with high probability. Suppose that \mathbf{X} is the data random variable, taking values in $(0, 1]^{m \times n}$. We are given M independent and identically distributed training samples $(\mathbf{X}_1, Q(\mathbf{X}_1)), \dots, (\mathbf{X}_M, Q(\mathbf{X}_M))$. We wish to use these training samples to learn the function Q , such that given $\epsilon \in (0, 1)$ and $\delta \in (0, 1)$, we have

$$\Pr_{\mathbf{X}_1, \dots, \mathbf{X}_M} \left(\Pr_{\mathbf{X}'} (\mathcal{A}((\mathbf{X}_i)_{i=1}^M, \mathbf{X}') \neq Q(\mathbf{X}')) \leq \epsilon \right) \geq 1 - \delta, \quad (7)$$

where $\mathcal{A}: ((0, 1]^{m \times n})^M \times (0, 1]^{m \times n} \rightarrow \{0, 1\}$ is an algorithm that takes the training data $\mathbf{X}_1, \dots, \mathbf{X}_M \in (0, 1]^{m \times n}$ as input and outputs the query function $\mathcal{A}((\mathbf{X}_i)_{i=1}^M, \cdot)$. Given training data $\mathbf{X}_1, \dots, \mathbf{X}_M \in (0, 1]^{m \times n}$, the quantity $\Pr_{\mathbf{X}'} (\mathcal{A}((\mathbf{X}_i)_{i=1}^M, \mathbf{X}') \neq Q(\mathbf{X}'))$ is the expected value of the 0-1 loss function (with respect to \mathbf{X}'). Note that for Equation (7) to hold, the number of samples M depends on ϵ , δ , and possibly other parameters in the problem. M can be interpreted as the number of queries required to learn the label assignments up to a small error with high probability.

Since the number of bins b is known to the decoding algorithm, it suffices to consider query functions of the form $h = h' \circ \Pi^{m \times n}$, where $h': [b]^{m \times n} \rightarrow \{0, 1\}$. Furthermore, we suppose that the data is binned before implementing the learning algorithm. Thus, we can write $\mathcal{A}(\cdot, \cdot) = \mathcal{A}'((\Pi^{m \times n})^M(\cdot), \Pi^{m \times n}(\cdot))$, where $\mathcal{A}': ([b]^{m \times n})^M \times [b]^{m \times n} \rightarrow \{0, 1\}$. Denote $\bar{\mathbf{X}} = \Pi^{m \times n} \circ \mathbf{X}$ to be the random variable taking values in $[b]^{m \times n}$, obtained by binning the entries of \mathbf{X} . Then, Equation (7) can be rewritten as

$$\Pr_{\bar{\mathbf{X}}_1, \dots, \bar{\mathbf{X}}_M} \left(\Pr_{\bar{\mathbf{X}}'} (\mathcal{A}'((\bar{\mathbf{X}}_i)_{i=1}^M, \bar{\mathbf{X}}') \neq Q'(\bar{\mathbf{X}}')) \leq \epsilon \right) \geq 1 - \delta, \quad (8)$$

For this reason, it suffices to assume that the input data corresponds to the labels of the bins.

E.1 VC dimension bounds for tabular data using query function of He et al. [2024]

In He et al. [2024], the z -score function is of the form $F_z(\mathbf{X}) = \beta_0 + \sum_{j=1}^n \beta_j T_j(\mathbf{X}) + \sum_{j=1}^n \alpha_j T_j(\mathbf{X})^2$, where for all i, j , we have $\beta_i, \alpha_j \in \mathbb{R}$ and $T_j(\mathbf{X})$ is the Hamming weight of the label string corresponding to the j th column of \mathbf{X} . As noted earlier in this section, it suffices to focus our attention to the case where the input is in $[b]^{m \times n}$, obtained by binning the original data. Our goal is to embed all possible query functions into a neural network and use known bounds on the VC dimension for learning the true query function.

Theorem E.1 (Query complexity bound for querying He et al. [2024] with tabular data). *Given the number of bins b , number of rows m and columns n of the query table, there is a neural network that can use*

$$O\left(\frac{mnb \log(mnb) \log(1/\epsilon) + \log(1/\delta)}{\epsilon}\right) \quad (9)$$

training data (labeled data consisting of query table and whether or not the table is watermarked according to He et al. [2024]), to learn the function which determines whether an input table is watermarked, with error at most $\epsilon > 0$ with respect to 0-1 loss (see Equation (8)), and with probability greater than or equal to $1 - \delta$ over the training samples.

Proof. We begin by embedding the labels $k \in [b]$ into vectors, so as to vectorize the inputs $[b]^{m \times n}$. To that end, associate the label $k \in [b]$ to the standard unit vector $\mathbf{e}_k \in \mathbb{R}^b$, where \mathbf{e}_k is the vector with 1 at the k th entry and zero elsewhere. Let $\mathbf{X} \in [b]^{m \times n}$ be the input data, and let it be mapped to the vector $\bigoplus_{j=1}^n \bigoplus_{i=1}^m \mathbf{e}_k \mathbf{x}_{ij}$. Here, the columns of \mathbf{X} are vertically stacked on top of each other after vectorizing.

Let $\mathbf{w} \in \{0, 1\}^b$ denote a candidate vector of labels. Observe that $\langle \mathbf{w}, \mathbf{e}_k \rangle = \mathbf{w}_k$ for all $k \in [b]$. Furthermore, for $j \in [n]$, we have $\langle \mathbf{w}^{\oplus m}, \bigoplus_{i=1}^m \mathbf{e}_k \mathbf{x}_{ij} \rangle = \sum_{i=1}^m \mathbf{w}_k \mathbf{x}_{ij}$. If \mathbf{w} is the correct labeling vector for the j th column, then $\sum_{i=1}^m \mathbf{w}_k \mathbf{x}_{ij} = T_j(\mathbf{X})$. By definition, we have $T_j(\mathbf{X}) \in [0, m]$ for all $j \in [n]$ and all $\mathbf{X} \in [b]^{m \times n}$.

Next, we show how to obtain $T_j(\mathbf{X})^2$ from $T_j(\mathbf{X})$. First, add another layer where we map $T_j(\mathbf{X})$ to $(m+1)T_j(\mathbf{X})$, by choosing the weight to be $m+1$. Next, choose the following piecewise polynomial activation function:

$$\psi(z) = \begin{cases} 0 & \text{if } z \leq 0 \\ z & \text{if } z \in (0, m] \\ z^2 & \text{if } z > m. \end{cases} \quad (10)$$

Then, since $T_j(\mathbf{X}) \in [0, m]$, we obtain $\psi(T_j(\mathbf{X})) = T_j(\mathbf{X})$. On the other hand, since $(m+1)T_j(\mathbf{X}) \in \{0\} \cup [m+1, m(m+1)]$, we obtain $\psi((m+1)T_j(\mathbf{X})) = (m+1)^2 T_j(\mathbf{X})^2$. The constant factor of $(m+1)^2$ can be absorbed into the weights in the next layer.

This motivates us to propose the following neural network architecture for the problem of learning the query function (see Figure 4). The input nodes contain vectorized indices, such that columns of \mathbf{X} are stacked on top of each other. Therefore, there are a total of mnb input nodes. The first hidden layer computes $T_1(\mathbf{X}), \dots, T_n(\mathbf{X})$. Since the $T_j(\mathbf{X}) \in [0, m]$ for all $j \in [n]$, the activation function acting on the first hidden layer does nothing. The second layer effectively fans out $T_j(\mathbf{X})$ for $j \in [n]$. The top node maps $T_j(\mathbf{X})$ to itself, whereas the bottom node maps $T_j(\mathbf{X})$ to $(m+1)T_j(\mathbf{X})$. Thus, applying the activation function at the second hidden layer gives us $T_j(\mathbf{X})$ and $(m+1)^2 T_j(\mathbf{X})^2$ for $j \in [n]$. The output layer is obtained by applying weights and biases to the second hidden layer. Thus, the output of the neural network is of the form $F_z(\mathbf{X}) = \beta_0 + \sum_{j=1}^n \beta_j T_j(\mathbf{X}) + \sum_{j=1}^n \alpha_j T_j(\mathbf{X})^2$. Since we need to compute the VC dimension, we

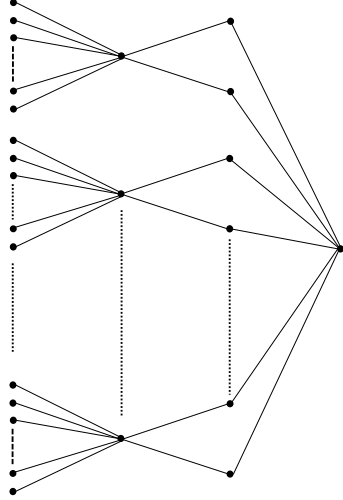


Figure 4: Neural network architecture to embed the problem of learning the query function. The activation function is applied at every node, except the nodes in the input and the output layers.

apply the sign (or indicator) function at the output layer. Therefore, the hypothesis class defined by this neural network is the set of functions computed by it over all the weights and biases at each layer, with a sign function (see (6)) applied at the end. By construction, all the query functions are a part of this hypothesis class. Thus, an upper bound on the VC dimension of the hypothesis class defined by the neural network also gives an upper bound on the VC dimension of the hypothesis class defined by all the query functions.

There are a total of $O(mnb)$ weight and bias parameters before the first layer, $O(n)$ parameters before the second layer, and finally, $O(n)$ parameters before the output layer. Thus, we have a total of $\text{wt} = O(mnb)$ parameters. We have a total of $L = 3$ layers. Let wt_i denote the number of weight and bias parameters from the input layer till the i th layer. Then, the effective depth of the neural network is $\bar{L} = \sum_{i=1}^L \text{wt}_i / \text{wt}$ is of order 1. Then, by [Bartlett et al., 2019, Theorem 6], the VC dimension of the neural network hypothesis class is bounded above by $O(mnb \log(mnb))$. Therefore, by [Shalev-Shwartz and Ben-David, 2014, Theorem 6.8], we can infer that

$$M = O\left(\frac{mnb \log(mnb) \log(1/\epsilon) + \log(1/\delta)}{\epsilon}\right) \quad (11)$$

training samples are sufficient to learn the query function to within an error of ϵ (with respect to the 0 – 1 loss) with probability greater than or equal to $1 - \delta$ over the training samples.

Now, denote $\mathcal{A}'(\text{training data}, \cdot)$ to be the query function that is learned from the training data. Then, if the distribution of the data is uniform, then $\Pr_{\bar{\mathbf{X}}'}(\mathcal{A}'(\text{training data}, \bar{\mathbf{X}}') \neq Q'(\bar{\mathbf{X}}'))$ is equal to the fraction of indices where the learned query function differs from the true query function. As a result, setting $\epsilon = 0.5/(mnb)$, we obtain the situation where we learn the query function exactly. Thus, we need $O((mnb)^2 \log(mnb) \log(b) + mnb \log(1/\delta))$ samples to learn the query function exactly with probability at least $1 - \delta$ over the training samples. \square

E.2 VC dimension bounds for tabular data using query function of Algorithm 1

Unlike He et al. [2024], in our work, we only watermark n columns of the input table (see Algorithm 1). Thus, during query time, one would need to identify first the columns of the query

table that are watermarked (referred to as value columns). As stated in Section 5, the query function returns 1 if the z -score of each of the value columns are greater than an input threshold $z_{\text{th}} \geq 0$. Thus, we prove the complexity of decoding Algorithm 1 for $\alpha \leq 0.5$ (which corresponds to $z_{\text{th}} \geq 0$).

Theorem E.2 (Query complexity bound for decoding Algorithm 1). *Given the number of bins b , number of rows m and columns $2n$ of the query table, and assuming that the significance level α for z -test in Section 5 is at most 0.5, there is a neural network that can use*

$$O\left(\frac{mnb \log(mnb) \log(1/\epsilon) + \log(1/\delta)}{\epsilon}\right) \quad (12)$$

training data (labeled data consisting of query table and whether or not the table is watermarked according to Algorithm 1), to learn the function which determines whether an input table is watermarked, with error at most $\epsilon > 0$ with respect to 0-1 loss (see Equation (8)), and with probability greater than or equal to $1 - \delta$ over the training samples.

Proof. Following the proof of Theorem E.1, we embed data $\mathbf{X} \in [b]^{m \times 2n}$ before feeding into a neural network. First, we embed the labels $k \in [b]$ into vectors, so as to vectorize the inputs $[b]^{m \times 2n}$. To that end, associate the label $k \in [b]$ to the standard unit vector $\mathbf{e}_k \in \mathbb{R}^b$, where \mathbf{e}_k is the vector with 1 at the k th entry and zero elsewhere. Let $\mathbf{X} \in [b]^{m \times 2n}$ be the input data, and let it be mapped to the vector $\bigoplus_{j=1}^{2n} \bigoplus_{i=1}^m \mathbf{e}_{\mathbf{X}_{ij}}$. Here, each column of each row of \mathbf{X} are vertically stacked on top of each other after vectorizing.

Now, our goal is to show that there is a neural network architecture with appropriate weights, biases, and activation function such that the output of the neural network is the true query function. The true query function outputs 1 *if and only if* the z -score of all the *value* columns is above the threshold z_{th} . As per Section 5, we denote the z -score of the j -th column as $z_j = 2(T_j(\mathbf{X})/\sqrt{m}) - \sqrt{m}$, for all $j \in [2n]$. For obtaining the true query function, we need to know which columns correspond to the value columns as well as which bins are watermarked in a given value column. Since we seek to embed the true query function into a neural network, we assume that we know the indices \mathcal{V} corresponding to the value column as well as the true labeling vectors. Algorithm 1, by design, ensures that $\mathcal{V} \subseteq [2n]$ and $|\mathcal{V}| = n$.

The first hidden layer contains a total of $2n$ nodes. Let $\mathbf{w} \in \{0, 1\}^b$ denote a candidate vector of labels (1 is interpreted as watermarked, while 0 is interpreted as not watermarked). Observe that $\langle \mathbf{w}, \mathbf{e}_k \rangle = \mathbf{w}_k$ for all $k \in [b]$. Furthermore, for all $j \in [n]$, we have $\langle \mathbf{w}^{\oplus m}, \bigoplus_{i=1}^m \mathbf{e}_{\mathbf{X}_{ij}} \rangle = \sum_{i=1}^m \mathbf{w}_{\mathbf{X}_{ij}}$. If $j \in \mathcal{V}$ and \mathbf{w} is the correct labeling vector for the j th column, then $\sum_{i=1}^m \mathbf{w}_{\mathbf{X}_{ij}} = T_j(\mathbf{X})$. Since $T_j(\mathbf{X}) \in [0, m]$, we add a bias of $\sqrt{m} + 1$ so that $T_j(\mathbf{X}) + \sqrt{m} + 1 > \sqrt{m}$. If, on the other hand, if $j \notin \mathcal{V}$, i.e., we have a key column, then we set the weight \mathbf{w} equal to the zero vector and add a bias of $m + \sqrt{m} + 2 > \sqrt{m}$. (We choose such a bias to internally distinguish a key column from a value column, since $T_j(\mathbf{X}) + \sqrt{m} + 1 < m + \sqrt{m} + 2$.) Subsequently, we apply the following piecewise-linear activation function:

$$\psi(x) = \begin{cases} 0 & \text{if } x \leq 0 \\ 1 + \frac{1}{2n} & \text{if } 0 \leq x \leq \sqrt{m} \\ x & \text{if } x > \sqrt{m}. \end{cases} \quad (13)$$

Then, the output of the first hidden layer (after applying the weights, biases, and activation function) is equal to $T_j(\mathbf{X}) + \sqrt{m} + 1$ if $j \in \mathcal{V}$, while it is equal to $m + \sqrt{m} + 2$ if $j \notin \mathcal{V}$.

For the second layer, our goal is to obtain the z -scores for the value columns and compare it to the threshold. To achieve this, we add a weight of $2/\sqrt{m}$ and a bias of $-\sqrt{m} - 2 - 2/\sqrt{m} - z_{\text{th}}$. Applying such a weight and bias to the value column $j \in \mathcal{V}$ gives $(2/\sqrt{m})(T_j(\mathbf{X}) + \sqrt{m} + 1) -$

$\sqrt{m} - 2 - 2/\sqrt{m} - z_{\text{th}} = z_j - z_{\text{th}}$, where z_j is the z -score of the j th column. Now, if $z_j - z_{\text{th}} \leq 0$ (or $z_j \leq z_{\text{th}}$), then the activation function outputs 0. On the other hand, if $z_j - z_{\text{th}} > 0$, then since $z_j \leq \sqrt{m}$ and $z_{\text{th}} \geq 0$ (as $\alpha \leq 0.5$ by assumption), we have $z_j - z_{\text{th}} \leq \sqrt{m}$, so that the activation function outputs $1 + 1/(2n)$. Note that for the *key* columns, we can set the weights as 1 and biases as 0. Then applying the activation function to these nodes, we have the output $m + \sqrt{m} + 2$ as before.

Finally, in the third layer (which is also the final/output layer), for each column corresponding to the values, we apply a weight of 1 and a bias of $-n$. For the key columns, we apply weight and bias equal to 0 (which is equivalent to ignoring the key columns at the final layer). Therefore, the output at the final layer is $\sum_{j \in \mathcal{V}} (1 + 1/(2n)) \mathbf{1}[z_j - z_{\text{th}} > 0] - n$, where $\mathbf{1}[A]$ denotes the indicator function of the event A (i.e., $\mathbf{1}[A] = 1$ if A is true and 0 otherwise). It can be verified that the output is positive if and only if $z_j > z_{\text{th}}$ for all $j \in \mathcal{V}$. Then, we apply the sign function given in (6) to this output. Thus, such a network can learn the true query function required. A schematic of the proposed neural network architecture is given in Figure 5.

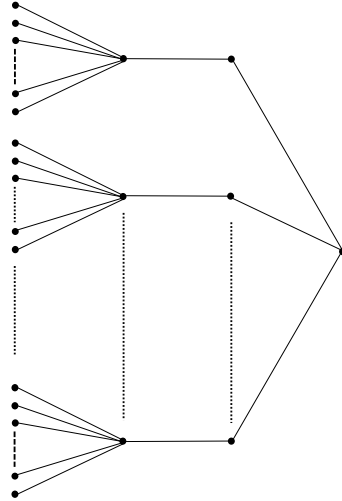


Figure 5: Neural network architecture to embed the problem of learning the query function for dataset watermarked according to Algorithm 1. The activation function is applied at every node, except the nodes in the input and the output layers.

The total number of parameters required to represent the weights and biases before the first layer is $O(mnb)$, before the second layer is $O(n)$, and before the third layer is $O(n)$. Thus we have a total of $O(mnb)$ parameters. We also have 3 layers in the architecture. The effective depth of our neural network is $O(1)$. Then, using [Bartlett et al., 2019, Theorem 6], the VC dimension of the neural network hypothesis class is bounded above by $O(mnb \log(mnb))$. Using [Shalev-Shwartz and Ben-David, 2014, Theorem 6.8],

$$M = O\left(\frac{mnb \log(mnb) \log(1/\epsilon) + \log(1/\delta)}{\epsilon}\right) \quad (14)$$

training samples are sufficient to learn the query function up to error ϵ with respect to the 0 – 1-loss with probability greater than or equal to $1 - \delta$ over the training samples.

Now, denote $\mathcal{A}'(\text{training data}, \cdot)$ to be the query function that is learned from the training data. Then, if the distribution of the data is uniform, then $\Pr_{\bar{\mathbf{X}}'}(\mathcal{A}'(\text{training data}, \bar{\mathbf{X}}') \neq Q'(\bar{\mathbf{X}}'))$ is equal to the fraction of indices where the learned query function differs from the true query

function. As a result, setting $\epsilon = 0.5/(mnb)$, we obtain the situation where we learn the query function exactly. Thus, we need $O((mnb)^2 \log(mnb) \log(b) + mnb \log(1/\delta))$ samples to learn the query function exactly with probability at least $1 - \delta$ over the training samples. \square

Corollary E.3 (Query complexity of row queries to both He et al. [2024] and Algorithm 1). *For queries of the form $\mathbf{X} \in \mathbb{R}^{m \times 1}$ and query function that computes $z = 2T(\mathbf{X})/\sqrt{m} - \sqrt{m}$ or any linear function of $T(\mathbf{X})$, there is a neural network that can learn this query function up to error ϵ in 0-1 loss using $O\left(\frac{mb \log(1/\epsilon) + \log(1/\delta)}{\epsilon}\right)$ samples with probability $1 - \delta$ over the training samples.*

Proof. Using $n = 1$ in Theorem E.2 gives us the result. For He et al. [2024], observe that when a single row is input, $T_j(\mathbf{X})$ for all $j \in n$ is in $\{0, 1\}$. As such, the statistical test uses z -score tests on the standard normal distribution, and not the χ^2 test. The hypothesis class corresponding to the neural architecture as defined in Theorem E.2 is thus PAC learnable for this problem, and so the query complexity bound follows by setting $n = 1$. \square

E.3 A lower bound for row queries to He et al. [2024] given the z -scores

Consider the case that the continuous space in $(0, 1]$ is uniformly discretized using bins of size $1/b$, i.e., construct bins in $(0, 1]$ as $-\{(0, \frac{1}{b}], (\frac{1}{b}, \frac{2}{b}], \dots, (\frac{b-1}{b}, 1]\}$. Then each of these bins are labeled $\{0, 1\}$ with some probability $1 - p$ and p respectively. We save this data-structure, and allow anyone to query it with $S \in (0, 1]^m$, responding with the z -score (Equation 3) and whether the data is watermarked or not. In this section, we want to bound the minimum number of queries one can make to the model and estimate the watermarking scheme with high accuracy. Specifically we ask:

When the number of bins b is known, what is the query complexity to correctly identify all red and green intervals used for watermarking?

Observe that for a row, the z -score is computed as: $2\sqrt{m} \left(\frac{T}{m} - \frac{1}{2} \right)$, where T is the number of values in the row falling in the bins with label 1.

When b is known to the adversary, the problem can be reduced to the 2-color Mastermind game. In 2-color mastermind the codemaker creates a secret code using a sequence of colored pegs, and the codebreaker guesses the sequence. At each query by the codebreaker, the codemaker provides the number of pegs they correctly guessed. As such, given z is the output of each query, one can easily compute the number of values in each bin $\{0, 1\}$. Thus, given any b , one can reduce this problem to the 2-color Mastermind game. This specific form of Mastermind has been extensively studied in the literature Chvátal [1983], Knuth [1976]. In particular, with 2 possible colors: red and green, the maximum number of row queries needed to recover the exact watermarking scheme is $\Theta\left(\frac{b \log(2)}{\log(b)}\right)$. Hence, the ‘red-green’ watermarking scheme by He et al. [2024] can be learned by an adversary making $\Theta\left(\frac{b \log(2)}{\log(b)}\right)$ queries to the detector. Note that this lower bound does not directly apply to the upper bounds derived using VC theory in Appendix E.1 and Appendix E.2, since here we assume access to the z -score for each query.